

DEVELOPMENT OF COMBINED FUNCTION MAGNETS FOR THE TAIWAN PHOTON SOURCE

C. Y. Kuo[#], C. S. Hwang and C. H. Chang, NSRRC, Hsinchu 30076, Taiwan

Abstract

Bending magnets, quadrupole magnets, and sextupole magnets are the most crucial magnetic elements in the synchrotron accelerator facility or high energy accelerator collider ring. Generally, separate bending magnets, quadrupoles or sextupoles magnets are utilized to perform separate functions. However, in the lattice design of accelerator ring or a compact ring in limited space, a single multifunction magnet is used to reduce the number of magnets and ensure that the entire device fits into the available space. This work presents an approach for designing the pole profiles of a combined-function bending magnet of the dipole, quadrupole, and sextupole components. The pole profile of a combined quadrupole magnet with gradient field and sextupole field components is also discussed.

INTRODUCTION

Combined function magnets [1] are utilized in several applied synchrotrons and beam lines. The magnetic field quality of such magnets depends mainly on the pole profile. Taiwan Photon Source (TPS) [2] has completed the design of combined function dipole and quadrupole magnets and the magnetic field of the TPS combined function magnets has been calculated using the TOSCA program. The defocusing quadrupole and sextupole field components are combined in the bending magnet. The gradient and sextupolar components are -1.7 T/m and -12.4 T/m², respectively, which are superimposed on the main dipole component of 0.819 T. The combined quadrupole is combined with sextupolar component that is employed in the minimization of geometrical aberrations. The sextupolar component reach 25.7 T/m², superimposed on the main quadrupole component of 11.3 T/m. This work presents profiles of the typical combined dipole and quadrupole magnets.

The calculated field $B(x)$ and the integral field $\int B(x)ds$ at the mid-plane are expressed using polynomial expansions as

$$B_x(x) + i B_y(x) = \sum_{n=0} (a_n / n!) x^n + i \sum_{n=0} (b_n / n!) x^n \quad (1)$$

$$\int B_x(x)ds + i \int B_y(x)ds = \sum_{n=0} (A_n / n!) x^n + i \sum_{n=0} (B_n / n!) x^n \quad (2)$$

where a_n and b_n denote the skew and normal components, respectively. The integral field normalization at the good field region x is defined as $|B_n/B_j| = (B_n/B_j)x^{(n-j)}$, in which j is the main component of each magnet and A_n and B_n are the integral skew and normal components.

COMBINED DIPOLE MAGNET

The field quality of most magnets depends mainly on the pole profile. The ideal pole profile of a dipole is a straight line that extends to infinity; the ideal profile of a quadrupole is a hyperbola. However, it is impossible to make an infinitely large dipole magnet. Therefore the width of the poles must be truncated to insert the current coils around the poles. Fig.1 presents the configuration of the combined function dipole. The upper-half cross section of the magnet is 320 mm wide and 100 mm high, with a pole width of 64 mm. The H type dipole magnet profile was designed to maintain a symmetric field and increase mechanical strength. The use of silicon steel (50CS1300) and the B-H data used in the calculations were based on a measured magnetization curve.

Dipole magnet coils made of copper have a square profile 13×13 mm² with a coolant orifice with a diameter of 6.5 mm. Table 1 presents the main magnet design parameters. When the pole gap is 24 mm at the center of dipole magnet and the current is 1034 A, the dipole field is 0.819 T. The pole profile equation combines $3x^2y - y^3 = R^3$ and $y = (2q/w)x$ to yield the main dipole, quadrupole and sextupole field strengths. Where q is 0.764 , the gradient component is -1.7 T/m, R is 6804 , the sextupolar component is -12.4 T/m², and w is 64 mm. The magnetic field was calculated using the TOSCA code.

Table 1: Magnet Specifications of Booster Ring Magnets

Type	Dipole BD/BF	Quadrupole QF
Quantity	42/12	48
Length (m)	1.6/0.8	0.3
Field strength(T, T/m, T/m ²)	0.819,-1.73,-12.4	11.3,26
Full gap (mm)	24	36
Good field range (mm)	±15	±15
Turns/pole	8	18
Conductor (mm ²)	13×13	5×5
Coolant diameter (mm)	6.5	2
Current (A)	1034	82
Power/magnet (kW)	6.4/3.3	0.14
Water circuit	2	2
Water velocity (m/s)	2.3/1.2	0.5
Voltage/magnet (V)	22/11.5	5.6

[#]kuo.cy@nsrrc.org.tw

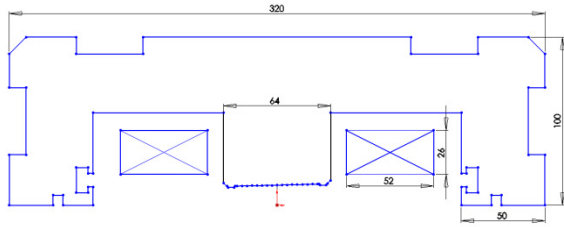


Figure 1: Cross-section view of combined dipole magnet.

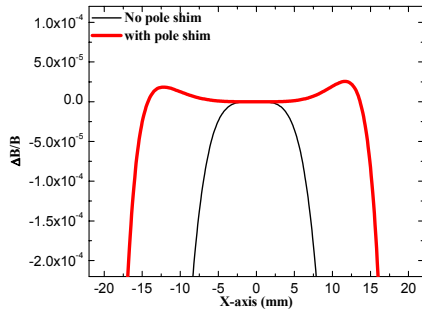


Figure 2: Field homogeneity of the central fields on the transverse x-axis; $\Delta B/B = [B(x) - (b_0 + b_1x + b_2x^2)]/B(x)$.

Figure 2 plots the deviation of the central field $\Delta B/B$: the black line represents the pole without shimming; the red line represents the pole with shims of various sizes. The end shims on the right and left sides of the pole have different sizes, increasing the good field region. The field quality $\Delta B/B$ in the good field region is within 0.005%.

Figure 3 shows the TOSCA 3D combined dipole model of length 1.566 m. The edge of the dipole magnet was chamfered by curved cutting to control the $[B_2ds]/[B_0ds]$ ratio. Table 2 presents the $[B_2ds]/[B_0ds]$ specifications. Before chamfering, the normalized integral multipole field error is shown in Fig. 4. The sextupole integral field exceeds the specified value of 5.28 T/m². End chamfer with dimensions of 2 mm at the end caps, applying a 45° cut to the pole tip to modify the $[B_2ds]/[B_0ds]$ ratio. Following chamfering, the normalized integral multipole field error is shown in Fig. 4 that the sextupole integral field error meets the specifications. Based on the integral dipole field strength of a magnet iron with a length of 1.566 m, an effective length of 1.6 m was obtained. Fig. 4 shows that the normalized integral multipole components of the combined dipole magnet at the normalization radius 15 mm are within 0.02%.

Table 2: Specification of Combined Dipole Integral Field

Type	L(m)	$[B_0ds]$	$[B_1ds]$	$[B_2ds]$	$[B_2ds]/[B_0ds]$
BD	1.6	1.31	-2.768	-19.84	15.1
BF	0.8	0.65	-1.384	-9.92	15.3

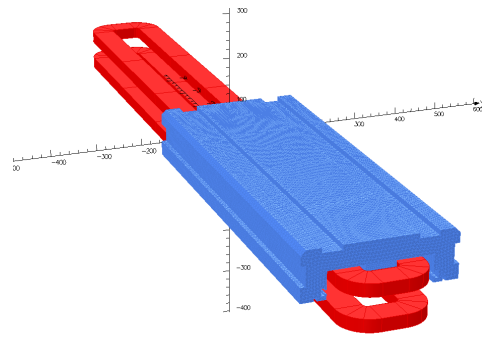


Figure 3: The TOSCA 3D combined dipole model.

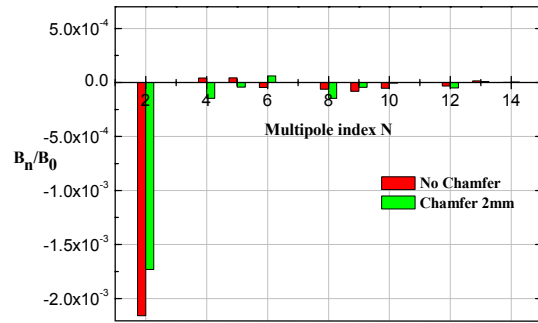


Figure 4: The normalization of the integral multipole components of the combined dipole magnet.

COMBINED QUADRUPOLE MAGNET

Figure 5 displays cross section of the combined function quadrupole of width 300 mm, height 150 mm and bore radius 18 mm. For ease of fabrication, the pole is designed at 65 degree between pole and the horizontal axis but the pole tip is maintained at 45 degree, and the coil easily assembles into the pole. The design and construction are based on assembly of the top and bottom to form a whole magnet. This method enables precise mechanical control and keeps the cost down. The coil of quadrupole magnet are made of copper have a square profile 5×5 mm² with a coolant hole of diameter 3 mm. The gap between the coil and the pole is only 0.8 mm. Table 1 lists the coil parameters that define the design of the quadrupole magnet.

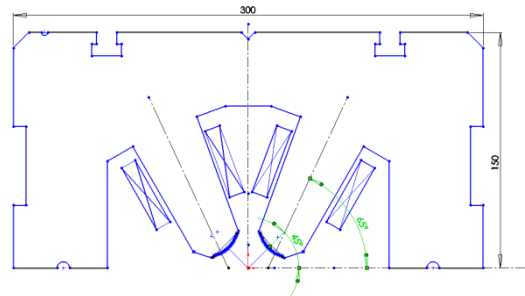


Figure 5: Cross-section view of quadrupole magnet.

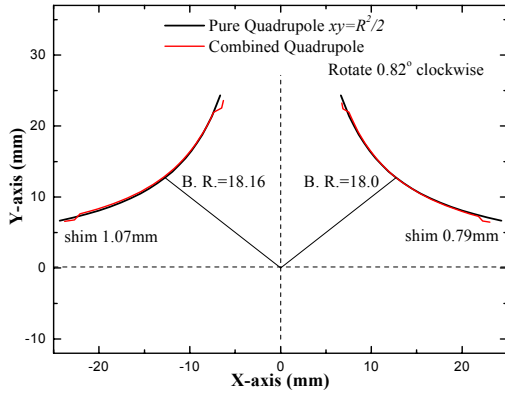


Figure 6: The pole profile detail of the combined quadrupole magnet.

Figure 6 depicts in detail the pole profile in Fig. 5. The pole profile equation $xy = R^2/2$ is the same as that for the pure quadrupole magnet, where R is 17.7 mm, such that the 20-pole strength can be reduced relative to that of the R is 18 mm. The combined quadrupole pole profiles are rotated through an angle of 0.82° clockwise in the top two quadrants to yield the preferred sextupole field strength. When the operating current density is 3.8 A/mm^2 and the cross section area of the coil is 450 mm^2 , the quadrupole field is 11.3 T/m . Rotating both poles through 0.82° generated a sextupolar component of 25.7 T/m^2 , but also produced an unwanted dipole field. Therefore the bore radius in the first quadrant is maintained at 18 mm, but that in the second quadrant moves 18.16 mm in the 135° direction to eliminate the dipole field strength. Different end shims are applied at the right (0.79 mm) and left (1.07 mm) poles to increase the good field region. Fig. 7 plots the field deviation of the central field $\Delta B/B$. The field quality $\Delta B/B$ in the good field region is within 0.005%.

Unlike the combined dipole, the combined quadrupole has chamfered removable end caps, with a 45° cut of a depth that is increased to 3.5 mm at the pole tip. Chamfering is applied to enhance the integral good field region and reduce the 12-pole strength, as presented in Fig. 8. With respect to the normalization of the integral field B_n/B_1 , Fig. 9 reveals that the normalized integral multipole components of the combined quadrupole magnet at a normalization radius of 15 mm is within 0.07%.

SUMMARY

Two typical combined function magnets were designed in this study. The main advantage of a combined function magnet is that it can be used in limited space in an accelerator facility and that it is relatively low-cost magnet. However, the evident disadvantage is that the bending, focusing and second-order correction cannot be separately controlled. Magnet chamfers can be used to set the $\int B_2 ds / \int B_0 ds$ of the combined dipole magnet and reduce the multipole errors of the combined quadrupole.

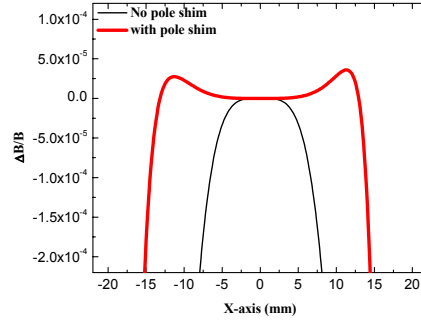


Figure 7: shows the field deviation of the central field; $\Delta B/B = [B(x) - (b_0 + b_1x + b_2x^2)]/B(x)$.

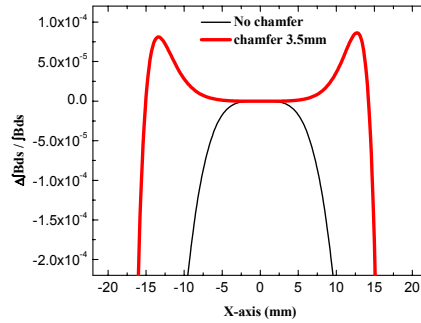


Figure 8: shows the field deviation of the integral field; $\Delta \int B ds / \int B ds = [\int B(x) ds - (B_0 + B_1x + B_2x^2)] / \int B(x) ds$.

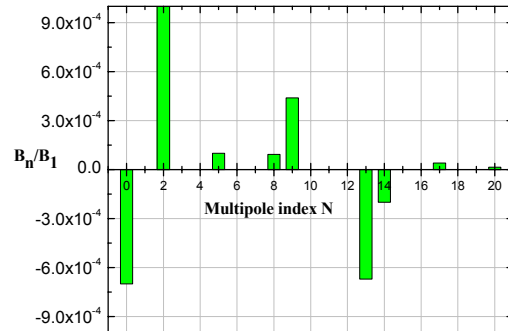


Figure 9: Normalization of the integral multipole components of the combined quadrupole magnet.

REFERENCES

[1] P. R. Sarma, et al., "New method of designing pole profile in combined function magnets of high field quality", Rev. Sci. Instrum. 70, p. 2655 (1999).
 [2] C. C. Kuo, et al., "Design of Taiwan future synchrotron light source", Proceedings of the EPAC'06, June 2006, p. 3445 (2006).